Research Square

Preprints are preliminary reports that have not undergone peer review.
They should not be considered conclusive, used to inform clinical practice,
or referenced by the media as validated information.

Mycoremediation of the Azo dye Acid Red 14 by Wickerhamomyces Anomalus: Physicochemical Characterization, Equilibrium, and Kinetics Studies

Mohammed Danouche (mohammed.danouche@usmba.ac.ma)
Université Sidi Mohamed Ben Abdellah https://orcid.org/0000-0003-1654-8372
Hicham El Arroussi
Mohammed VI Polytechnic University (UM6P)
Naima El Ghachtouli
Mohammed VI Polytechnic University (UM6P)

Research Article

Keywords: Wickerhamomyces anomalus, Azo dye, Biosorption, Kinetic and Isotherms model, Biomass characterization, Optimization

Posted Date: September 20th, 2021

DOI: https://doi.org/10.21203/rs.3.rs-891092/v1

License: This work is licensed under a Creative Commons Attribution 4.0 International License.
Read Full License

Mycoremediation of the azo dye Acid Red 14 by *Wickerhamomyces anomalus:* Physicochemical characterization, equilibrium, and kinetics studies

Danouche M.[1,2 *], El Arroussi H.[1,3], El Ghachtouli N. [2]

[1] *Green Biotechnology Center, Moroccan Foundation for Advanced Science, Innovation and Research (MAScIR), Rabat, Morocco.*

[2] *Microbial Biotechnology and Bioactive Molecules Laboratory, Sciences and Technologies Faculty, Sidi Mohamed Ben Abdellah University, Fez, Morocco.*

[3] *AgroBioScience (AgBS), Mohammed VI Polytechnic University (UM6P), Ben Guerir, Morocco*

[*]Correspondence: mohammed.danouche@usmba.ac.ma

ORCID ID (Danouche M.): https://orcid.org/0000-0003-1654-8372

ORCID ID (El Ghachtouli N): https://orcid.org/0000-0002-5452-5406

ORCID ID (El Arroussi H.): https://orcid.org/0000-0001-7964-5538

Acknowledgements

The authors gratefully acknowledge the Moroccan Foundation for Advanced Science, Innovation and Research (MAScIR), and Regional University Centre of Interface (CURI), Sidi Mohamed Ben Abdellah University for their financial and technical support.

Authors contribution statement

Danouche M. : Conceptualization, Methodology, Formal analysis, Writing - original draft, Visualization.

El Arroussi H. : Supervision, Writing - review & editing, Resources.

El Ghachtouli N. : Supervision, Conceptualization, Writing - review & editing, Validation, Funding acquisition, Project leading.

Abstract

This study aimed to evaluate the potential application, and the involved mechanism in the biosorption of Acid Red$_{14}$ (AR$_{14}$) by the biomass of *Wickerhamomyces anomalus.* Kinetics and biosorption isotherms were first examined. Then, the physicochemical characterization of cells-AR$_{14}$ interactions was determined using scanning electron microscopy coupled with energy dispersive X-ray spectroscopy, Fourier transforms infrared spectroscopy, zeta potential, zero-point charge, and contact angle measurements. Finally, the Plackett-Burman and the Box-Behnken designs were used respectively to identify the most influential factors on the biosorption process and their optimization. The pseudo-second-order and the intra-particle diffusion models best fit the experimental data. Furthermore, the Langmuir model was the appropriate isotherm to explain the biosorption system, suggesting the involvement of chemisorption on a monolayer of homogeneous sites. Biomass characterizations supported these theoretical predictions. A change in the transmittance of the functional groups present was noticed after AR14-biosorption, the analysis of the zeta potential confirms the presence of anionic groups, and the contact angle measurement indicates a significant variation of the electron donor and acceptor character. Hence, it can be concluded that both chemical and electrostatic interactions of AR14 onto the macromolecular structures composing the cell surface. The most influential factors on biosorption efficiency were dye and biomass concentration, and the pH of the medium. Optimal biosorption was achieved at pH 3-4, with AR14 concentrations around 50 - 75 mg L^{-1} and a biomass concentration at 1.25 g L^{-1}. These results suggest that *W. anomalus* might be exploited as an effective, inexpensive, and environmentally friendly biosorbent.

Keywords: *Wickerhamomyces anomalus*; Azo dye, Biosorption; Kinetic and Isotherms model; Biomass characterization; Optimization.

1. Introduction

Worldwide, the textile industry is one of the leading fast-growing businesses. However, for the production of 1 kg of finished textile products, this manufacturing requires between 200 to 500 L of water, which makes this sector one of the largest producers of liquid effluents (Waghmode et al. 2012). It has also been estimated that approximately 10 000 tons per year of synthetic dyes are used in this sector, of which 10-15% are rejected during the dyeing process as waste (Saratale et al. 2011). Unfortunately, the release of these effluents into the aquatic environment does not only affect the color of the water, also it has adverse effects on exposed organisms, including humans (Fu and Viraraghavan 2001). To deal with this issue, strict regulations have been implemented to manage the release of such xenobiotics into the environment. Also, several approaches have been proposed as solutions for their treatment, such as membrane, photochemical oxidation, and electrochemical processes. Although these methods are effective, they require chemicals, energy-intensive equipment, and require high maintenance costs. Which makes them expensive, thereby limiting their large-scale applications (Arslan et al. 2016). Recently, there has been a particular interest in new technologies that are environmentally friendly, efficient, and inexpensive such as adsorption techniques. Activated carbon is the most commonly used adsorbent material (Yagub et al. 2014). However, their thermal or chemical regeneration as well as the need for complexing agents to improve their performance make the use of activated carbon-based processes an expensive proposition (Crini et al. 2019). New economical, readily available and effective adsorbents are in high demand today. Hence, the use of biological materials (biosorbents) such as natural residues, industrial food wastes, agricultural wastes, and biomass of various microorganisms has been reported as a cheap and effective alternative (Srinivasan and Viraraghavan 2010). Several studies have been reported the potential application of microalgae,

cyanobacteria, and filamentous fungi in the biosorption of toxic dyes (Aksu and Tezer 2005; Jafari et al. 2014; Rita de Cássia et al. 2013). However, only a few studies have focused on yeast cells, despite their advantages over other taxa. Particularly their fast growth compared to filamentous fungi or microalgae (Singh and Arora 2011), their ability to survive in harsh environments (Sen et al. 2016), and the special flocculating characteristic that allows them to aggregate into multicellular masses (flakes), facilitating, therefore, their recovery after the treatment process (Soares and Soares 2012). The purpose of this study was to evaluate the potential application of inactivated cells of *Wickerhamomyces anomalus* (*W. anomalus*) in the biosorption of the dye Acid red 14 (AR14). The specific objectives of this research were: (i) to study the kinetics and equilibrium isotherms of the biosorption of the AR14 dye by yeast cells. (ii) to investigate the physicochemical interaction between the yeast biomass and the dye, and (iii) to optimize the biosorption process using the design of the experiments.

2. Material and methods

2.1 Chemicals

The monoazo dye AR14 (1-Naphthalenesulfonic acid, 4-hydroxy-3-((4-sulfo-1-naphthalenyl) azo)-, disodium salt), commonly employed in many different industries such as textile, paper, food, etc..., was used as a model pollutant. The dye solution was prepared at a concentration of 5 g L^{-1} in distilled water, then sterilized by filtration and store at 4 ºC. All other chemicals used for this study were of analytical grade reagents and were purchased from Sigma and Merck.

2.2 Yeast source, culture medium, and biosorbent preparation

This study was conducted with the heat-kill cells of *W. anomalus* yeast strain, previously isolated from a contaminated site located in Fez (Morocco). Its pure culture was maintained on Yeast

Extract–Peptone–Glucose (YPG) medium (2% Difco peptone, 1% yeast extract, and 2% glucose) (Bahafid et al. 2013). The biomass was recovered by centrifugation at 10,000xg. and inactivated by autoclaving (121ºC for 45 min). The regression equation of OD_{600nm} and the dry cell weight (DCW) was calculated based on the standard curve according to eq (1).

$$DCW = 0.2418 \times OD_{600nm} + 0.2609 \quad (R^2 = 0.989) \qquad \text{eq (1).}$$

2.3 Biosorption: kinetics and equilibrium study

Kinetic studies were carried out in Erlenmeyer flasks containing 150 mL of the dye solution at a concentration of 50 mg L^{-1} and 0.5 g L^{-1} of biomass. The flasks were placed on orbital shakers at a constant speed (120 rpm) at 25 ºC. Aliquots were collected at a regular time, centrifuged (10 000xg for 10 min) to remove the biosorbent, and the dye concentration was measured using the spectrophotometer Prim Light SECOMAM at $\lambda = 515$ nm. The biosorption was reported as decolorization rate (D%) (eq 2), and the biosorption capacity was calculated according to eq 3.

$$D\% = (A(i) - A(t)) / A(i) \times 100 \qquad \text{eq (2).}$$

$$Qt = ((C(i)-C(t))\ V / W) \qquad \text{eq (3).}$$

Where, (Qt) is the biosorption capacity, A(i) and A(t) are the absorbance of dye dopped medium at the start point (i) and at a regular time (t); C(i) and C(t) are the initial and the equilibrium dye concentrations (mg L^{-1}); V is the volume of the solution (mL); W is the weight of the biomass (g L^{-1}). To explain and predict the kinetics of the yeast-dye biosorption interaction, various mathematical kinetic and isotherm models can be employed (Danouche et al. 2021). In this study, Lagergren's Pseudo-first-order and pseudo-second-order were applied to define the type of interactions (physisorption or chemisorption), while the intra-particle diffusion model was used to describe the internal diffusion of dye in the cell wall. The isotherms were next employed to describe the biosorption efficiency and to understand the relationship between the dye concentrations at its

equilibrium concentration in the biosorbent solution (Morosanu et al. 2016). The linear equations of kinetic and isotherm models used in the present study are summarized in Table 1.

2.4 Physicochemical characterization of W. anomalus / dye interaction

2.4.1 Scanning electron microscopy with energy dispersive X-Ray analysis

SEM (JSM-IT500 InTouchScope™) was used to visualize the surface morphology of cells from control and AR14 dopped medium, while EDX was used to analyze the elemental composition of control and AR14-loaded cells in the imaged area. The SEM analytical settings were as follows: Signal SED, magnification of x1 000-x55 000 landing voltage of 3.0 kV, operation distance of 10.1 mm, at high vacuum mode.

2.4.2 Fourier-transform infrared spectroscopy analysis

In order to determine the functional groups on the surface of *W. anomalus* and their participation in the biosorption of AR14. Control and AR14-loaded cells were analyzed by ABB Bomem FTLA 2000 spectrometer analyzer. Salt pellets were prepared using 1 mg of biomass and 149 mg of KBr. Samples were dried at 85 ºC for 24 h and compressed at 40 kN for 5 min to form pellets. Thirty-two scans were performed at a range of 400 to 4000 cm^{-1}, with 4 cm^{-1} of resolution for each sample.

2.4.3 Zeta potential and Zero-point charge measurement

The zeta potential measurement was performed to determine the zeta potentials of the yeast cell as a function of pH from 3 to 10. Indeed, a volume of 100 mL of yeast suspension (0.05 g L^{-1}) was harvested by centrifugation at 10 000xg for 10 min, then the biomass was resuspended in 10 mL of 0.1 M NaCl. The initial pH of the suspensions was adjusted from 3 to 10 with 0.1 M of HCl or NaOH solutions. Next, the zeta potential was evaluated in the electrophoresis cell at 25 ºC with

Nanosizer Nano (Malvern). For each pH value, triplicate measurements were taken, and for each data, approximately 30 readings were taken (Hadjoudja et al. 2010). The electrical state of the yeast surface in the solution was also characterized using the zero-charge point (pHzc). Indeed, NaCl solutions (0.1 M) with pH ranging from 3 to 10 were prepared, before being mixed with 0.05 g of the fungal biomass, and then were shaken for 24 h at 25 ºC. Finally, the final pH values were measured and the difference in ΔpH was plotted against the initial pHi to determine the pHzc (Zehra, et al. 2016).

2.4.4 Contact angle measurement

Measurement of the contact angle was carried out at 25 ºC as described by Asri et al. (2018), using a digital optical contact angle (Data Physics OCA 40), via the sessile drop method, using water, formamide, and diiodomethane (Table S1). Both the left and the right contact angles measurements of algal biomasses were automatically calculated from the digitalized image using SCA 20 software. The degree of hydrophobicity of control and dye-leaded to cells of *W. anomalus* was then estimated according to Vogler's and Van Oss approach (Van Oss, et al 1988; Vogler 1998).

2.5 Statistical analysis

Experiments were carried out in triplicate, and the results were recorded as the mean ± standard deviation. The statistical analysis of obtained data was performed using GraphPad Prism software version 8.0, with an unpaired T-test. P-value of < 0.05 was perceived as statistically.

2.6 Optimization of biosorption using the design of experiments

2.6.1 Screening of factors using Plackett–Burman design (PBD)

Factors screening was performed using PBD (Plackett and Burman 1946) via MINITAB 18.1 software. The selection of the most influential factors on the biosorption process was based on previous research addressing biosorption optimization using a "one factor at a time" approach. Indeed, six variables were selected including temperature (ºC), pH, yeast biomass (g L^{-1}), dye concentration (mg L^{-1}), shaking speed (rpm), and contact time (min) at two levels (max (+1) and min (-1)) (Table S2). According to the adopted method, it was presumed that there is no interaction between parameters. Therefore, the data were modeled using first-order multiple regression (eq 7).

$$Y = \beta_0 + \sum \beta_i X_{i\ (i = 1, ..., k)} \quad \text{eq (7).}$$

Where, (Y) is the biosorption response, (β_0) is the model intercept, and (β_i) is the variable estimates. Thus, ANOVA and lack of fit were used for statistical significance. While the Fisher variation ratio (F), and the P-value (P) were used to select the effective parameters.

2.6.2 Optimization of biosorption parameters using Box-Behnken design (PBD)

To optimize the biosorption of AR14 by the biomass of *W. anomalus*, the PBD model was applied (Box and Behnken 1960). The eq (8) was used to calculate the coded values of variables.

$$Xi = (x_i - x_0 / \Delta x),\ i = 1, 2, 3, \ldots k \quad \text{eq (8).}$$

Where, (Xi) is the dimensionless value of a process variable; (x_i) is the real value of an independent variable; (x_0) is the value of (x_i) at the center point; (Δx) is the step change. The second-order equation (eq (9)) was used to correlate the dependent and independent variables:

$$Y = b_0 + b_1A + b_2B + b_3C + b_{12}AB + b_{13}AC + b_{23}BC + b_{11}A^2 + b_{22}B^2 + b_{33}C^2 \quad \text{eq (9).}$$

Where, (Y) is the biosorption efficiency response; (b_0) is constant, (b_1, b_2, and b_3) are linear coefficients; (b_{12}, b_{13}, and b_{23}) are cross-product coefficients, and (b_{11}, b_{22}, and b_{33}) are quadratic coefficients; (A, B, and C) are coded experimental levels of the selected variables of the screening phase. It was represented in terms of three class levels (low (-1), central point (0), and high (+1))

178 (Table S3). The optimum values of each factor were calculated by solving the regression equation,
179 evaluating the contour map, and setting up constraints on the variable levels (Kousha et al. 2012).
180 The significance of the model is derived from the test of goodness-of-fit, mostly expressed as the
181 coefficient of determination (R^2). A P-value below 0.05 was considered statistically significant
182 (Papadopoulou et al. 2013).

183 ## 3. Results and discussion

184 ### *3.1 Biosorption: kinetics and equilibrium study*

185 The result of AR14 biosorption kinetics in *W. anomalus* biomass at four initial dye concentrations
186 (50, 100, 150, and 200 mg L^{-1}) indicates that the rate of biosorption increased with increasing the
187 contact time up to 10 min, after that, an equilibrium was reached (Fig. 1). Indeed, three phases were
188 recorded in this biosorption process. The initial phase (5 min), a rapid biosorption rate occurred.
189 Afterward, the dye is gradually biosorbed until the maximum biosorption capacity of the
190 biosorbents is reached. The initial phase can be attributed to the availability of a large surface area
191 and many vacant macropores for the dye uptake. Also, the fast dye biosorption at this phase
192 suggesting the involvement of a passive interaction like physical adsorption or ion exchange
193 interaction. The second stage (5 to 10 min), was characterized by a gradual and slow absorption,
194 explained by the saturation of active functions groups on the cell surface (Daneshvar et al. 2019).
195 As well as, by the repulsive forces among adsorbed dye molecules and those present in the solution
196 (Smaranda et al. 2009). At the third stage, the biosorption reached the equilibrium state. Similar
197 findings were reported previously on the biosorption of Strazone blue (Farah et al. 2007), Acid
198 blue 161 (Dilarri et al. 2016), and Direct red 23 (Morão et al. 2017) using various *S. cerevisiae*
199 biomass.

200 The pseudo-second-order model was more applicable for the AR14-yeast biosorption system fit.
201 Indeed, there was a linearization of the experimental data (Fig. 2A), and the R^2 of all studied
202 concentrations was relatively close to 1 (Table 2). Moreover, the calculated values of Qe (cal) were
203 closer to the experimental values Qe (exp), confirming the goodness-of-fit of the model. The
204 distinguishing features of this model are related to the biosorption capacity of the solid phase,
205 which is in agreement with chemosorption (Davranche et al. 2019). However, the pseudo-second-
206 order model did not identify the potential mechanism of diffusion into the pores. The kinetics were
207 then analyzed through the intraparticle diffusion model. It has been shown that if biosorption
208 follows an intraparticle diffusion model, the plot of (Qt) versus ($\sqrt{t}$) should be linear, and if the plot
209 passes through the origin (C = 0). However, if (C # 0), this point to some degree of boundary layer
210 control. The intraparticle diffusion model is not the rate control step of the biosorption process, but
211 it can work simultaneously with other diffusion models (Wu et al. 2009). As shown in Fig. 2B, two
212 linear regions are representing the diffusion boundary layer, followed by intraparticle diffusion in
213 macropore (Ho and McKay 1998). This result highlights that the yeast biomass reaches biosorption
214 equilibrium when diffusion occurs in the macropore layer, and the resistance to mass transfer is not
215 involved in the dye uptake kinetics (Ka Yee et al. 2003). Also, Kismir and Aroguz (2011) reported
216 that the process of mass transfer of dye onto the biosorbents can take place in general through four
217 steps: (i) bulk diffusion (transfer from the bulk solution to the surface of the biosorbent), (ii) film
218 diffusion (transfer through the boundary layer to the biosorbent surface), (iii) intra-particle
219 diffusion (transfer from the surface to the interior pores of the particle), (iv) chemical reaction via
220 ion-exchange, complexation, chelation; the adsorption of dye at an active site on the biosorbent
221 surface. According to the graphical representation of Langmuir and Freundlich isotherms (Fig. 3),
222 and the corresponding models' constants listed in Table 3, the R^2 was respectively at 0.954 and

223 0.849. Which means that Langmuir isotherms provide an appropriate fit for AR14 biosorption onto
224 *W. anomalus* compared to Freundlich isotherms. Langmuir isotherms predict that the biosorption
225 is based on monolayer adsorption on a homogeneous site, without any interaction between
226 biosorbed dye molecules on neighboring sites, it also assumes that the energy is equal for all sites
227 and that there are multiple biosorption sites for a specific surface. When these sites are fully
228 saturated, no further biosorption can take place (de Castro et al. 2017; Daneshvar et al. 2019). Aksu
229 and Dönmez (2003) reported the applicability of both Langmuir and Freundlich models to the
230 biosorption system of Remazol Blue reactive dye into dried cells of *Candida* strains.

231 ### *3.2 Characterization of yeast biomass*

232 #### *3.2.1 SEM coupled with EDX analysis*

233 SEM and EDX analysis were used to establish the changes in morphology and the elemental
234 composition of the yeast biomass before AR14 biosorption, in order to establish the binding
235 mechanism of the dye to the cell wall. Fig. 4A shows the SEM images of colorless yeast cells, and
236 Fig. 4B shows *W. anomalus* after AR14 biosorption. There was a difference in cellular morphology
237 between the control and AR14-loaded cells. The yeast cells before biosorption of AR14 had a
238 normal shape and a transparent outer layer outside the cell surface. However, after dye biosorption,
239 the cell becomes smooth and presents hazy textures. Furthermore, the X-ray spectra showed a
240 difference in the intensity of elementary peaks of C, O, P, and K after dye biosorption.

241 #### *3.2.2 FTIR spectroscopy analysis*

242 The FTIR spectra (Fig. 5) of *W. anomalus* biomass before and after AR14 biosorption were used
243 to identify the involved functional groups of the cell wall in the dye-biosorption process
244 (Pugazhenthi 2009). The strong vibration around 3000–3500 cm^{-1} illustrates the existence of

245 stretching vibration of hydroxyl (-OH) and/or amino (-NH_2) groups, which are among the
246 functional groups of chitosan and amino acids on the cell wall of *W. anomalus* (Paula et al. 2016).
247 The peaks at 2854 – 2923 cm^{-1} are in the region of the absorption of lipid acyl chains (3050-2800
248 cm^{-1}) that correspond to symmetric and asymmetric stretching of methylene and methyl groups in
249 the membrane phospholipids (Ami et al. 2014). The strong peaks at 1642 cm^{-1} detected in the region
250 between 1700 and 1500 cm^{-1} indicate the presence of amide (I and II) bands, mainly from protein
251 peptide bonds (C=O stretching and N-H bending), corresponding to several uronic acids and amino
252 acids present in the cell wall (Zhang et al. 2010). The infrared absorption in the spectral at 1406
253 cm^{-1} may be caused by the sulfur (-SO-) and phosphorous (-PO-) groups, which range between
254 1500 and 1300 cm^{-1} corresponding to vibrations of fatty acids and proteins (Paula et al. 2016). The
255 bands observed at 1073 cm^{-1} are assigned to C-O stretching vibration of alcohols and carboxylic
256 acids which are mainly related to complex vibrations from carbohydrates (Naja and Volesky 2011).
257 Based on the comparison of the spectra before and after biosorption, a significant change was
258 noticed in the transmittance of these functional groups which may be attributed to its occupation
259 by dye molecule. There was also a shift in various bands, which represented the groups involved
260 in the biosorption corresponding to hydroxyl, carboxylic acid, amine, and amino groups. Some
261 previous studies indicated that the biosorption process is accomplished by chelation and formation
262 of ionic bridges between dye and functional groups. The binding mechanism of dye molecules to
263 the yeast cell is explained by the strong attractive forces of peptidomannan, peptidoglycan, lipids,
264 and heteropolysaccharides…, which contains several functional groups such as carboxyl, hydroxyl,
265 amino, phosphate, and other charged groups (Gadd 2009; Vitor and Corso 2008). In line with our
266 findings, it has been reported by Dilarri et al. (2016) that the biosorption of synthetic dyes by the
267 cell wall of *S. cerevisiae* involved some amide and amine groups, and demonstrated that the

vibration of (-C=O) and (-C-O) can be another linking group in the chitin structure. Moreover, it can be predicted according to the FTIR analysis that Yoshida H-binding, dipole-dipole H-binding, π-π, and n-π interactions play an indispensable role in the AR14 biosorption onto yeast cell (Tran et al. 2017). The cell wall architecture and the proposed mechanisms of AR14 biosorption are illustrated in Fig. 6. In fact, the major components of the *S. cerevisiae* cell wall are β-glucans (formed by 1,3-β- and 1,6-linkages) and mannoproteins (proteins highly N- or O-glycosylated mannose residues linked by 1,2,-1,3-, 1,4- and 1,6-α-linkages), which represent about 50-60% and 40-50%, respectively of the cell wall mass, as well as 1-3% for the chitin, which is manufactured by 1,4-β-N-acetylglucosamine (Stewart 2017). These complex macromolecular structures present potential binding sites for diverse pollutants including toxic dye molecules (Fomina and Gadd 2014).

3.2.3 Zeta potential and Zero-point charge measurement

The electrical state of the cell surface is one of the critical parameters in biosorption studies. Thus, the measurement of zeta potential can be one of the key parameters related to the external loads of the adsorbent (Akar et al. 2009). As shown in Fig. 7A, the zeta potential of *W. anomalus* biomass was maintained at a negative charge, regardless of the initial pH value, and it varied from –4.6 mV at pH 3 to -9.28 at pH 10. This can testify to the anionic characteristics and the high concentration of acid functional groups on the surface of *W. anomalus*. These results are consistent with previous studies that evaluated the zeta potential of different yeast strains (Lin et al. 2003; Tazhibaeva et al. 2003). It is known that there was a close relationship between the zeta potential of biomaterials and their biosorption capacity (Dundar et al. 2008). On the other hand, the value of pHzc at which ΔpH = 0 was found at 5.25 (Fig. 7B) confirmed thus the presence of anionic groups on the cell surface that dominate over the cationic groups. Zehra et al. (2016) reported that the acidic value of pHzc

of baker's yeast, was attributed to the presence of various biopolymers on the yeast cell wall, mainly β-glucan and chitosan, that may have caused a substantial load on the external surface of the cells and given a net charge on the surface that depending on the pH caused by deprotonation of functional groups in the cell wall (Garcia-rubio et al. 2020; Klis et al. 2002). The number of positively charged sites decreases when the pH of the solution increases. The decrease in the biosorption of AR14 anions is a result of the electrostatic repulsion forces of the negatively charged cell surface at acidic pH conditions (Akar et al. 2009).

3.2.4 Contact angle measurements

Based on both Vogler's and Van Oss approaches, *W. anomalus* exhibited a hydrophilic character, the θ_w value (34.9 ° ± 0.4) was less than 65 °, and the ΔGiwi had a positive value (37.23 ± 1.13 mJ m^{-2}). These findings agree with previous results reporting the hydrophilic character of various yeast strains (Lucas et al. 2006; Guillemot et al. 2006). The hydrophobicity of the yeast surface has been attributed to the proteins forming the cell wall (Suzzi et al. 1994; Vichi et al. 2010). In addition, *W. anomalus* appear to behave predominantly as electron donors/Lewis bases with high values of γ^- = 52.57 ± 0.6 mJ m^{-2} (Table 4). These results also indicate that this strain exhibits weak electron acceptor characters with γ^+ = 0.24 ± 0.07 mJ m^{-2}. Some previous research reported also that the microbial cell surfaces are mainly electron-donating, while electron-accepting cell surfaces are rarely found (Mei et al. 1998), which may be due to the presence of phosphate groups in the cell wall (Vichi et al. 2010). These findings are consistent with the FTIR analyses of *W. anomalus,* which confirm the presence of phosphate groups on its cell surface. On the other hand, the θ_w of *W. anomalus* significantly decreased from 34.9 ° ± 0.4 to 31.6 ° ± 0.9 after dye biosorption (Table 4). This may be attributed to an increase in the density of polar functional groups on the biomass surfaces after the biosorption process (Legorreta-Castañeda et al. 2020). In addition, a significant

variation was noted in the electron donor and acceptor character after dye biosorption (γ^+ from 0.24 ± 0.07 to 0.08 ± 0.02 mJ m^{-2}; and γ^- from 52 57 ± 0.6 to 59.79 ± 0.5 mJ m^{-2}) which can be attributed to the interaction of cell surface functional groups with dye molecules.

3.3 Optimization of the biosorption by using the design of experiments

3.3.1 Factor's screening using Plackett–Burman design

Based on the positive or negative values of the factors modeled on the eq 10, both factors A and C have positive values, indicating their synergistic effect on the biosorption, while the other negative factors indicate an antagonistic effect.

$$D\ \% = 11.0 + 0.933\ A - 3.64\ B + 12.89\ C - 0.003\ D - 0.207\ E + 0.774\ F \quad \text{eq (10).}$$

Table 5 represents the value of the regression coefficients, the t-tests, and the p-values of six independent variables. The multiple correlation coefficient R^2 of the first-order model indicates that 75.82% of the data variance could be estimated by this model. Moreover, the difference between the predicted R2 (51.80%) and the adjusted R2 (67.28%), indicates that the relationship between the independent variables and the response cannot be evaluated based on the first-order model. As illustrated in Fig. 8A, the significant influence factors on biosorption capacity are the biomass (89.06%), pH (26.57%), and the dye concentration (10.94%). Indeed, the increase in the yeast dosage showed a positive influence, while increasing dye concentration and pH had a negative influence on the efficiency of AR14 biosorption (Fig. 8B).

Several studies reported that an increase in biomass dosage significantly improves the biosorption capacity, due to the increase of exchangeable sites present in the cell wall (Kousha et al. 2012). pH is also one of the factors controlling the biosorption process. In fact it can affect the chemistry of dye molecules, the physicochemical properties of the yeast surface, and the magnitude of

electrostatic charges imparted by the ionized dye molecules (Fu and Viraraghavan 2002). It has been documented that the optimal biosorption pH of particular dyes depends closely on their chemical properties. For instance, the biosorption of reactive dyes require acidic conditions, whereas basic dyes biosorption require neutral or alkaline conditions (Farah et al. 2007). In addition, the net charge of the biosorbent is also pH-dependent, at a low pH value, the functional group on the cell surface becomes protonated and acquires a net positive charge increasing thereby the binding of anionic dyes.

Regarding the effect of the initial dye concentration on the biosorption capacity, its closely depending on the binding sites available on the biomass surface. Moreover, it has been reported that a high dye solute uptake can be obtained at a high initial dye concentration, which is linked to the high driving force for mass transfer (Binupriya et al. 2007; Bulut and Aydin 2006). However, at lower initial dye concentrations, the biosorption becomes independent of the initial dye concentration, because the ratio of the initial moles of the solute to the available area becomes low (Vijayaraghavan and Yun 2008).

3.3.2 Optimization of process parameters using Box-Behnken model

The eq (11) models the relationship between the predicted biosorption response and the process parameters with the second-order polynomial equation. In fact, the negative values of both factors (A) and (C) indicate that a high biosorption efficiency occurs at lower dye concentration and at acidic pH solution.

$$D\% = 70.8 - 0.243\,A + 48.99\,B - 23.18\,C - 0.00015\,A^*A - 10.50\,B^*B + 1.625\,C^*C + 0.0001\,A^*B + 0.0419\,A^*C - 2.61\,B^*C \quad \text{eq (11).}$$

As illustrated in Table 6, the regression of the quadratic model was statistically significant (F=21.48; P=0.00), at 95% confidence limits. The R^2 indicate that the model as fitted explains 90.62% of the variability, suggesting a significant correlation between the predicted and experimental effects of the selected variables. Furthermore, the predicted R^2 value (76.27%) was in line with the founded R^2value (86.41%) of the adjusted, indicating that 10.14% of the variability in the response was not explainable by this model. Also, the F value was significantly proportional to the pure error, and the F values for the factors A, B and C were at 17.44, 42.69, and 79.62, respectively, showing consequently that the pH of the solution was most significantly different from zero at the 95.0% confidence level followed by the biomass dosage and dye concentration (Fig. 9A). Consistent with the results of the factor selection step, the normalized effects indicate that increasing the yeast dose had a positive influence, whereas a negative influence on biosorption efficiency was observed when increasing the dye concentration or initial pH of the medium (Fig. 9B). As described in Fig. 10A, the contours illustrating the change in AR14 biosorption, relative to the simultaneous change in two factors. while the third is included at the midpoint. When the initial pH was maintained at 5, the biosorption rate was proportional to the increase in the biomass dosage, but inversely proportional to the increase in the initial dye concentration. Meanwhile, when the initial dye concentration was maintained at 125 mg L^{-1} (Fig. 10B), the rate of biosorption was proportional to the increase in the biomass dosage, and the optimum biosorption was achieved at a lower pH level. Similarly, when the biomass dosage was maintained at 1.125 mg L^{-1} (Fig. 10C), the optimum biosorption level was proportional to the initial pH of the medium and the initial dye concentration. Higher biosorption was achieved at acidic conditions with lower dye concentration. El-Naggar and El-Malkey (2020) reported that the dye biosorption system depended on protonation or deprotonation of the functional groups on the cell surface. At pH 3-4, the protonation of amino

groups on the yeast cell wall increases the net positive charge and enhances the biosorption of negatively charged dye ions by electrostatic binding.

4. Conclusion

Based on the above considerations, it can be concluded that the biomass of *W. anomalus* could be used as an effective, inexpensive and environmentally friendly biosorbent for the removal of toxic dyes. The study of the kinetics of biosoprtopn indicated that at the beginning of the biosorption process, the bioremoval occurred rapidly, then proceeded gradually to reach the equilibrium state. The studied isotherm model indicated a monolayer adsorption of AR14 molecules at homogeneous sites on the cell wall surface of *W. anomalus*. Furthermore, biosorption kinetic modelling followed both the pseudo-second-order as well as the intraparticle diffusion model. The characterization of yeast biomass before and after dye biosorption indicated that the bioremoval was attributed to the presence of various active groups on the cell surface, the zeta potential of *W. anomalus* was at a negative charge, and the acidic value of pHzc confirmed the presence of anionic groups on the cell surface that dominate over the cationic groups. The adsorbate concentration and the adsorbent dosage ratio as well as the initial pH have significantly affected the biosorption efficiency. The optimum condition for maximum dye biosorption was achieved at pH 3-4, with lower initial dye concentrations (50 - 75 mg L^{-1}) and yeast biomass greater than 1.25 g L^{-1}. Until today, very few studies have been conducted on the use of yeasts as biosorbent. To our knowledge, most of these researches are limited to the laboratory scale. Hence the emergence of this new research topic which may be part of the future solutions proposed for the treatment of colored effluents.

Compliance with ethical standards

Conflict of interest

The authors declare that they have no direct or indirect conflict of interest.

Ethical approval

This is the original work of the authors. The work described has not been submitted elsewhere for publication, in whole or in part, and all authors listed carried out the data analysis and manuscript writing. Moreover, all authors read and approved the final manuscript.

Data Availability

All data generated or analysed during this study are available from the corresponding author.

Funding

Not Applicable

References

Akar, Tamer, Burcu Anilan, Asli Gorgulu, and Sibel Tunali. (2009). Assessment of Cationic Dye Biosorption Characteristics of Untreated and Non-Conventional Biomass : *Pyracantha Coccinea Berries*. *Journal of Hazardous Materials* 168: 1302–9. https://doi.org/10.1016/j.jhazmat.2009.03.011.

Akar, S. T., Gorgulu, A., Kaynak, Z., Anilan, B., and Akar, T. (2009). Biosorption of Reactive Blue 49 Dye under Batch and Continuous Mode Using a Mixed Biosorbent of Macro-Fungus *Agaricus Bisporus* and *Thuja Orientalis* Cones. *Chemical Engineering Journal* 148: 26–34. https://doi.org/10.1016/j.cej.2008.07.027.

Aksu, Zümriye, and Gönül Dönmez. (2003). A Comparative Study on the Biosorption Characteristics of Some Yeasts for Remazol Blue Reactive Dye. *Chemosphere* 50(8): 1075–83. https://doi.org/10.1016/S0045-6535(02)00623-9.

Aksu, Zümriye, and Sevilay Tezer. (2005). Biosorption of Reactive Dyes on the Green Alga *Chlorella vulgaris*. *Process Biochemistry* 40(3–4): 1347–61. https://doi.org/10.1016/j.procbio.2004.06.007.

Ami, D., Posteri, R., Mereghetti, P., Porro, D., Doglia, S. M., and Branduardi, P. (2014). Fourier Transform Infrared Spectroscopy as a Method to Study Lipid Accumulation in Oleaginous Yeasts. *Biotechnology for Biofuels*: 7–12. https://doi.org/https://doi.org/10.1186/1754-6834-7-12.

Arslan, Serkan, Murat Eyvaz, Ercan Gürbulak, and Ebubekir Yüksel. (2016). A Review of State-of-the-Art Technologies in Dye- Containing Wastewater Treatment – The Textile Industry Case. In *Textile Wastewater Treatment*, InTech, 3–28. https://doi.org/http://dx.doi.org/10.5772/64140.

Asri, M., El Ghachtouli, N., Elabed, S., Koraichi, S. I., Elabed, A., Silva, B., and Tavares, T. (2018). *Wicherhamomyces Anomalus* Biofilm Supported on Wood Husk for Chromium Wastewater Treatment. *Journal of Hazardous Materials* 359(May): 554–62. https://doi.org/10.1016/j.jhazmat.2018.05.050.

Bahafid, W., Joutey, N. T., Sayel, H., Iraqui-Houssaini, M., and El Ghachtouli, N. (2013). Chromium Adsorption by Three Yeast Strains Isolated from Sediments in Morocco. *Geomicrobiology Journal* 30(5): 422–29. https://doi.org/10.1080/01490451.2012.705228.

Binupriya, A. R., Sathishkumar, M., Kavitha, D., Swaminathan, K., and Yun, S. E. (2007). Aerated and Rotated Mode Decolorization of a Textile Dye Solution by Native and Modified Mycelial Biomass of *Trametes Versicolor*. *Journal of Chemical Technology and Biotechnology* 82(4): 350–359. https://doi.org/10.1002/jctb.

445 Box, G.E.P., and D.W. Behnken. (1960). Some New Three Level Design for Study of Quantitative
446 Variables. *Technometrics* 2: 455-475. https://doi.org/10.2307/1266454

447 Bulut, Yasemin, and Haluk Aydin. (2006). A Kinetics and Thermodynamics Study of Methylene
448 Blue Adsorption on Wheat Shells. *Desalination* 194(1–3): 259–67.
449 https://doi.org/10.1016/j.desal.2005.10.032.

450 de Castro, Ketinny Camargo, Aline Silva Cossolin, Hélen Cristina Oliveira dos Reis, and Eduardo
451 Beraldo de Morais. (2017). Biosorption of Anionic Textile Dyes from Aqueous Solution by
452 Yeast Slurry from Brewery. *Brazilian Archives of Biology and Technology* 60(December): 1–
453 13. https://doi.org/10.1590/1678-4324-2017160101.

454 Crini, Grégorio, Eric Lichtfouse, Lee D. Wilson, and Nadia Morin-Crini. (2019). Conventional and
455 Non-Conventional Adsorbents for Wastewater Treatment. *Environmental Chemistry Letters*
456 17(1): 195–213. https://doi.org/10.1007/s10311-018-0786-8.

457 Daneshvar, Ehsan, Arya Vazirzadeh, and Amit Bhatnagar. (2019). Biosorption of Methylene Blue
458 Dye onto Three Different Marine Macroalgae: Effects of Different Parameters on Isotherm,
459 Kinetic and Thermodynamic. *Iranian Journal of Science and Technology, Transaction A:*
460 *Science* 43(6): 2743–54. https://doi.org/10.1007/s40995-019-00764-8.

461 Danouche, M., El Arroussi, H., Bahafid, W., and El Ghachtouli, N. (2021). An Overview of the
462 Biosorption Mechanism for the Bioremediation of Synthetic Dyes Using Yeast Cells.
463 *Environmental Technology Reviews* 10(1): 58–76.
464 https://doi.org/10.1080/21622515.2020.1869839.

465 Davranche, M., Veclin, C., Pierson-Wickmann, A. C., El Hadri, H., Grassl, B., Rowenczyk,L., Dia,
466 A., Halle, A.T. Blancho, F., Reynaud, S., and Gigault, J. (2019). Are Nanoplastics Able to

Bind Significant Amount of Metals? The Lead Example. *Environmental Pollution* 249: 940–48. https://doi.org/10.1016/j.envpol.2019.03.087.

Dilarri, Guilherme, Érica Janaina Rodrigues de Almeida, Hengli Barbosa Pecora, and Carlos Renato Corso. (2016). Removal of Dye Toxicity from an Aqueous Solution Using an Industrial Strain of *Saccharomyces Cerevisiae* (Meyen). *Water, Air, and Soil Pollution* 227(8). http://dx.doi.org/10.1007/s11270-016-2973-1.

Dundar, Murat, Cigdem Nuhoglu, and Yasar Nuhoglu. (2008). Biosorption of Cu (II) Ions onto the Litter of Natural Trembling Poplar Forest. *J. Hazard. Mater*. 151 86–95. https://doi.org/10.1016/j.jhazmat.2007.05.055.

El-Naggar, N. E. A., Rabei, N. H., and El-Malkey, S. E. (2020). Eco - Friendly Approach for Biosorption of - Pb 2 + and Carcinogenic Congo Red Dye from Binary Solution onto Sustainable *Ulva Lactuca* Biomass. *Scientific Reports* (0123456789): 1–22. https://doi.org/10.1038/s41598-020-73031-1.

Farah, Joseph Y, Nour Sh El-Gendy, and Laila A Farahat. (2007). Biosorption of Astrazone Blue Basic Dye from an Aqueous Solution Using Dried Biomass of Baker's Yeast. *Journal of hazardous materials* 148(1–2): 402–8. https://doi.org/10.1016/j.jhazmat.2007.02.053.

Fomina, Marina, and Geoffrey Michael Gadd. (2014). Biosorption: Current Perspectives on Concept, Definition and Application. *Bioresource Technology* 160: 3–14. http://dx.doi.org/10.1016/j.biortech.2013.12.102.

Fu, Yuzhu, and T. Viraraghavan. (2001). Fungal Decolorization of Dye Wastewaters: A Review. *Bioresource Technology* 79: 251–62. https://doi.org/10.1556/034.58.2016.1-2.6.

488 Fu, Yuzhu, and T. Viraraghavan. (2002). Removal of Congo Red from an Aqueous Solution by
489 Fungus *Aspergillus Niger. Advances in Environmental Research* 7(1): 239–47.
490 https://doi.org/10.1016/S1093-0191(01)00123-X.

491 Gadd, Geoffrey Michael. (2009). Biosorption: Critical Review of Scientific Rationale,
492 Environmental Importance and Significance for Pollution Treatment. *Journal of Chemical*
493 *Technology and Biotechnology* 84(1): 13–28. https://doi.org/10.1002/jctb.1999.

494 Garcia-Rubio, R., de Oliveira, H. C., Rivera, J., and Trevijano-Contador, N. (2020). The Fungal
495 Cell Wall : *Candida , Cryptococcus* , and *Aspergillus* Species. *Frontiers in microbiology*, 10
496 (2993): 1–13. https://doi.org/10.3389/fmicb.2019.02993.

497 Hadjoudja, S, V Deluchat, and M Baudu. (2010). Cell Surface Characterisation of *Microcystis*
498 *Aeruginosa* and *Chlorella Vulgaris*. *Journal of Colloid And Interface Science* 342(2): 293–
499 99. http://dx.doi.org/10.1016/j.jcis.2009.10.078.

500 Ho, Y. S., and G. McKay. (1998). Kinetic Models for the Sorption of Dye from Aqueous Solution
501 by Wood. *Process Safety and Environmental Protection* 76(2): 183–91.
502 https://doi.org/10.1205/095758298529326.

503 Jafari, Narjes, Mohammad Reza Soudi, and Rouha Kasra-Kermanshahi. (2014). Biodecolorization
504 of Textile Azo Dyes by Isolated Yeast from Activated Sludge: *Issatchenkia Orientalis* JKS6.
505 *Annals of Microbiology* 64(2): 475–82. https://doi.org/10.1007/s13213-013-0677-y

506 Ka Yee, Ho, Gordon McKay, and Yeung King Lun. (2003). Selective Adsorbents from Chemically
507 Modified Ordered Mesoporous Silica. *Langmuir* 19(7): 3019–24.
508 https://doi.org/10.1016/s0167-2991(04)80581-0.

509 Kismir, Yasemin, and Ayse Z. Aroguz. (2011). Adsorption Characteristics of the Hazardous Dye
510 Brilliant Green on Sakli{dotless}kent Mud. *Chemical Engineering Journal* 172(1): 199–206.
511 https://doi.org/10.1016/j.cej.2011.05.090.

512 Klis, F. M., P. Mol, K. Hellingwerf, and S. Brul. (2002). Dynamics of Cell Wall Structure in
513 *Saccharomyces cerevisiae*. *FEMS Microbiology Reviews* 26. https://doi.org/10.1111/j.1574-
514 6976.2002.tb00613.x

515 Kousha, M., Daneshvar, E., Dopeikar, H., Taghavi, D., and Bhatnagar, A. (2012). Box-Behnken
516 Design Optimization of Acid Black 1 Dye Biosorption by Different Brown Macroalgae.
517 *Chemical Engineering Journal* 179: 158–68. http://dx.doi.org/10.1016/j.cej.2011.10.073.

518 Legorreta-Castañeda, A. J., Lucho-Constantino, C. A., Beltrán-Hernández, R. I., Coronel-Olivares,
519 C., and Vázquez-Rodríguez, G. A. (2020). Biosorption of Water Pollutants by Fungal Pellets.
520 *Water*, 12(4), 1155. doi:10.3390/w12041155

521 Lin, D. Q., Brixius, P. J., Hubbuch, J. J., Thömmes, J., and Kula, M. R. (2003). Biomass/Adsorbent
522 Electrostatic Interactions in Expanded Bed Adsorption: A Zeta Potential Study. *Biotechnology*
523 *and bioengineering* 83(2): 149-157. https://doi.org/10.1002/bit.10654.

524 Lucas, M. S., Amaral, C., Sampaio, A., Peres, J. A., and Dias, A. A. (2006). Biodegradation of the
525 Diazo Dye Reactive Black 5 by a Wild Isolate of *Candida Oleophila*. *Enzyme and Microbial*
526 *Technology* 39(1): 51–55. https://doi.org/10.1016/j.enzmictec.2005.09.004.

527 Mei, H C Van Der, R Bos, and H J Busscher. (1998). A Reference Guide to Microbial Cell Surface
528 Hydrophobicity Based on Contact Angles. *Colloids and Surfaces B: Biointerfaces* 11(4): 213–
529 21. https://doi.org/doi:10.1016/s0927-7765(98)00037-x.

Rita de Cássia, M., de Barros Gomes, E., Pereira Jr, N., Marin-Morales, M. A., Machado, K. M. G., and de Gusmão, N. B. (2013). Biotreatment of Textile Effluent in Static Bioreactor by Curvularia Lunata URM 6179 and *Phanerochaete Chrysosporium* URM 6181. *Bioresource Technology* 142: 361–67. http://dx.doi.org/10.1016/j.biortech.2013.05.066.

Morão, Luana Galvão, Guilherme Dilarri, and Carlos Renato Corso. (2017). Immobilization of *Saccharomyces Cerevisiae* Cells on *Luffa Cylindrica*: A Study of a Novel Material for the Adsorption of Textile Dye. *Water, Air, and Soil Pollution* 228(7): 228–48. https://doi.org/10.1007/s11270-017-3433-2.

Morosanu, I., Teodosiu, C., Paduraru, C., Ibanescu, D., and Tofan, L. (2016). Biosorption of Lead Ions from Aqueous Ef Fl Uents by Rapeseed Biomass. *New Biotechnology*. http://dx.doi.org/10.1016/j.nbt.2016.08.002.

Naja, Ghinwa, and Bohumil Volesky. (2011). *The Mechanism of Metal Cation and Anion Biosorption. In Microbial Biosorption of Metals (Pp. 19-58).* Dordrecht: Springer.

Van Oss, C. J., M. K. Chaudhury, and R. J. Good. (1988). Interfacial Lifshitz-van Der Waals and Polar Interactions in Macroscopic Systems. *Chemical reviews* 88(6): 927–41. https://doi.org/10.1021/cr00088a006.

Papadopoulou, Konstantina, Iphigeneia Maria Kalagona, Antonios Philippoussis, and Fotis Rigas. (2013). Optimization of Fungal Decolorization of Azo and Anthraquinone Dyes via Box-Behnken Design. *International Biodeterioration and Biodegradation* 77: 31–38. http://dx.doi.org/10.1016/j.ibiod.2012.10.008.

A. Paula, G. Maria, A. Gabriela, F. Zielinski, M. Vieira, C. Windson, I. Haminiuk. (2016). Biosorption of Anthocyanins from Grape Pomace Extracts by Waste Yeast : Kinetic and

552 Isotherm Studies. *Journal of Food Engineering* 169: 53–60.
553 https://doi.org/10.1016/j.jfoodeng.2015.08.016.

554 Plackett, R. L., Burman, J. P. (1946). The design of optimum multifactorial experiments.
555 Biometrika, 33(4), 305–325. https://doi.org/doi:10.2307/2332195.

556 Pugazhenthi, P Monash G. (2009). Adsorption of Crystal Violet Dye from Aqueous Solution Using
557 Mesoporous Materials Synthesized at Room Temperature. : 390–405.
558 https://doi.org/10.1007/s10450-009-9156-y

559 Saratale, R. G., G. D. Saratale, J. S. Chang, and S. P. Govindwar. (2011). Bacterial Decolorization
560 and Degradation of Azo Dyes: A Review. *Journal of the Taiwan Institute of Chemical*
561 *Engineers* 42(1): 138–57. https://doi.org/10.1016/j.jtice.2010.06.006

562 Sen, Sudip Kumar, Smita Raut, Partha Bandyopadhyay, and Sangeeta Raut. (2016). Fungal
563 Decolouration and Degradation of Azo Dyes: A Review. *Fungal Biology Reviews* 30(3): 112–
564 33. http://dx.doi.org/10.1016/j.fbr.2016.06.003.

565 Singh, Kamaljit, and Sucharita Arora. (2011). Removal of Synthetic Textile Dyes from
566 Wastewaters: A Critical Review on Present Treatment Technologies. *Critical Reviews in*
567 *Environmental Science and Technology* 41(9): 807–78.
568 https://doi.org/10.1080/10643380903218376

569 Smaranda, Camelia, Dumitru Bulgariu, and Maria Gavrilescu. (2009). An Investigation of the
570 Sorption of Acid Orange 7 from Aqueous Solution onto Soil. *Environmental Engineering and*
571 *Management Journal* 8(6): 1391–1402. https://doi.org/10.30638/eemj.2009.203

572 Soares, Eduardo V., and Helena M.V.M. Soares. (2012). Bioremediation of Industrial Effluents

573 Containing Heavy Metals Using Brewing Cells of *Saccharomyces Cerevisiae* as a Green
574 Technology: A Review. *Environmental Science and Pollution Research* 19(4): 1066–83.

575 Srinivasan, Asha, and Thiruvenkatachari Viraraghavan. (2010). Decolorization of Dye
576 Wastewaters by Biosorbents: A Review. *Journal of Environmental Management* 91(10):
577 1915–29. http://dx.doi.org/10.1016/j.jenvman.2010.05.003.

578 Stewart, G. G. (2017). The Structure and Function of the Yeast Cell Wall , Plasma Membrane and
579 Periplasm. In *Brewing and Distilling Yeasts*, Springer, Cham., 55–75.
580 https://doi.org/https://doi.org/10.1007/978-3-319-69126-8_5.

581 Suzzi, Giovanna, Patrizia Romano, and Lucia Vannini. (1994). Cell Surface Hydrophobicity and
582 Flocculence in *Saccharomyces Cerevisiae* Wine Yeasts '. *Colloids and Surfaces B:*
583 *Biointerfaces* 2: 505–10. https://doi.org/10.1016/0927-7765(94)80058-8

584 Tazhibaeva, S M, K B Musabekov, A B Orazymbetova, and A A Zhubanova. (2003). Surface
585 Properties of Yeast Cells. *Colloid Journal* 65(1): 122–24.
586 https://doi.org/https://doi.org/10.1023/A:1022391613491.

587 Tran, Nguyen Hai, Sheng-jie You, and Ahmad Hosseini-bandegharaei. (2017). Mistakes and
588 Inconsistencies Regarding Adsorption of Contaminants from Aqueous Solutions : A Critical
589 Review. *Water Research* 120: 88–116. http://dx.doi.org/10.1016/j.watres.2017.04.014.

590 Guillemot, G., Vaca-Medina, G., Martin-Yken, H., Vernhet, A., Schmitz, P., and Mercier-Bonin,
591 M. (2006). Shear-Flow Induced Detachment of *Saccharomyces Cerevisiae* from Stainless
592 Steel : Influence of Yeast and Solid Surface Properties. *Colloids and Surfaces B: Biointerfaces*
593 49: 126–35. https://doi.org/10.1016/j.colsurfb.2006.03.001.

Vichi, S., Gallardo-Chacón, J. J., Pradelles, R., Chassagne, D., López-Tamames, E., and Buxaderas, S. (2010). Surface Properties of *Saccharomyces Cerevisiae* Lees during Sparkling Wine Ageing and Their Effect on Flocculation. *International Journal of Food Microbiology* 140(2–3): 125–30. http://dx.doi.org/10.1016/j.ijfoodmicro.2010.04.009.

Vijayaraghavan, K., and Yeoung Sang Yun. (2008). Bacterial Biosorbents and Biosorption. *Biotechnology Advances* 26(3): 266–91. https://doi.org/10.1016/j.biotechadv.2008.02.002.

Vitor, Vivian, and Carlos Renato Corso. (2008). Decolorization of Textile Dye by *Candida Albicans* Isolated from Industrial Effluents. *Journal of Industrial Microbiology and Biotechnology* 35(11): 1353–57. https://doi.org/10.1007/s10295-008-0435-5.

Vogler, Erwin A. (1998). Structure and Reactivity of Water at Biomaterial Surfaces. *Advances in Colloid and Interface Science* 74: 69–117. https://doi.org/10.1016/S0001-8686(97)00040-7

Waghmode, Tatoba R., Mayur B. Kurade, Akhil N. Kabra, and Sanjay P. Govindwar. (2012). Degradation of Remazol Red Dye by *Galactomyces Geotrichum* MTCC 1360 Leading to Increased Iron Uptake in *Sorghum Vulgare* and *Phaseolus Mungo* from Soil. *Biotechnology and Bioprocess Engineering* 17(1): 117–26. https://doi.org/10.1007/s12257-011-0307-0.

Wu, Feng Chin, Ru Ling Tseng, and Ruey Shin Juang. (2009). Initial Behavior of Intraparticle Diffusion Model Used in the Description of Adsorption Kinetics. *Chemical Engineering Journal* 153(1–3): 1–8. https://doi.org/10.1016/j.cej.2009.04.042.

Yagub, Mustafa T, Tushar Kanti Sen, Sharmeen Afroze, and H M Ang. (2014). Dye and Its Removal from Aqueous Solution by Adsorption: A Review. *Advances in colloid and interface science* 209: 172–84. https://doi.org/10.1016/j.cis.2014.04.002.

615 Zehra, Tasneem, Namal Priyantha, and Linda B.L. Lim. (2016). Removal of Crystal Violet Dye
616 from Aqueous Solution Using Yeast-Treated Peat as Adsorbent: Thermodynamics, Kinetics,
617 and Equilibrium Studies. *Environmental Earth Sciences* 75(4): 1–15.
618 https://doi.org/10.1007/s12665-016-5255-8.

619 Zhang, Y., Liu, W., Xu, M., Zheng, F., and Zhao, M. (2010). Study of the Mechanisms of Cu 2 +
620 Biosorption by Ethanol / Caustic-Pretreated Baker ' s Yeast Biomass. *Journal of Hazardous*
621 *Materials* 178(1–3): 1085–93. http://dx.doi.org/10.1016/j.jhazmat.2010.02.051.

622 ***Figure captions***

623 Fig 1. Kinetics of AR14 uptake by *W. anomalus* biomass at various initial dye concentrations.

624 Fig 2. Plot of pseudo-second order model (A), and intra-particle diffusion model (B) of AR14
625 biosorption onto *W. anomalus* at various initial concentrations.

626 Fig 3. Langmuir (A) and Freundlich (B) isotherm plot and fitted models of AR14 biosorption by
627 *W. anomalus* biomass.

628 Fig 4. SEM of *W. anomalus* (x8000): (A) control yeast cells; (B) dye loaded, and the selected X-
629 ray spectra of control (C), and dye loaded cells (D).

630 Fig 5. FTIR spectra of *W. anomalus* cells before and after AR14 biosorption.

631 Fig 6. Architecture of yeast cell wall and proposed interaction mechanisms of AR14 biosorption

632 Fig 7. Zeta potential of (A) and pH zero charge (B) of *W. anomalus* yeast cells.

633 Fig 8. Main effect of variables on the biosorption capacity of AR14 using *W. anomalus*: Pareto
634 chart of standard effect (A), and normal plot of standardized effects (B).

635 Fig 9. Effect of variables and 2-way interaction on the biosorption capacity of AR14 using *W.*
636 *anomalus*: pareto-chart of standardized effects (A), and normal plot of standardized effects (B).

637 Fig 10. Effect of selected factors (pH, dye concentration, and yeast biomass) on the biosorption
638 capacity of AR14 onto *W. anomalus*

639

Figures

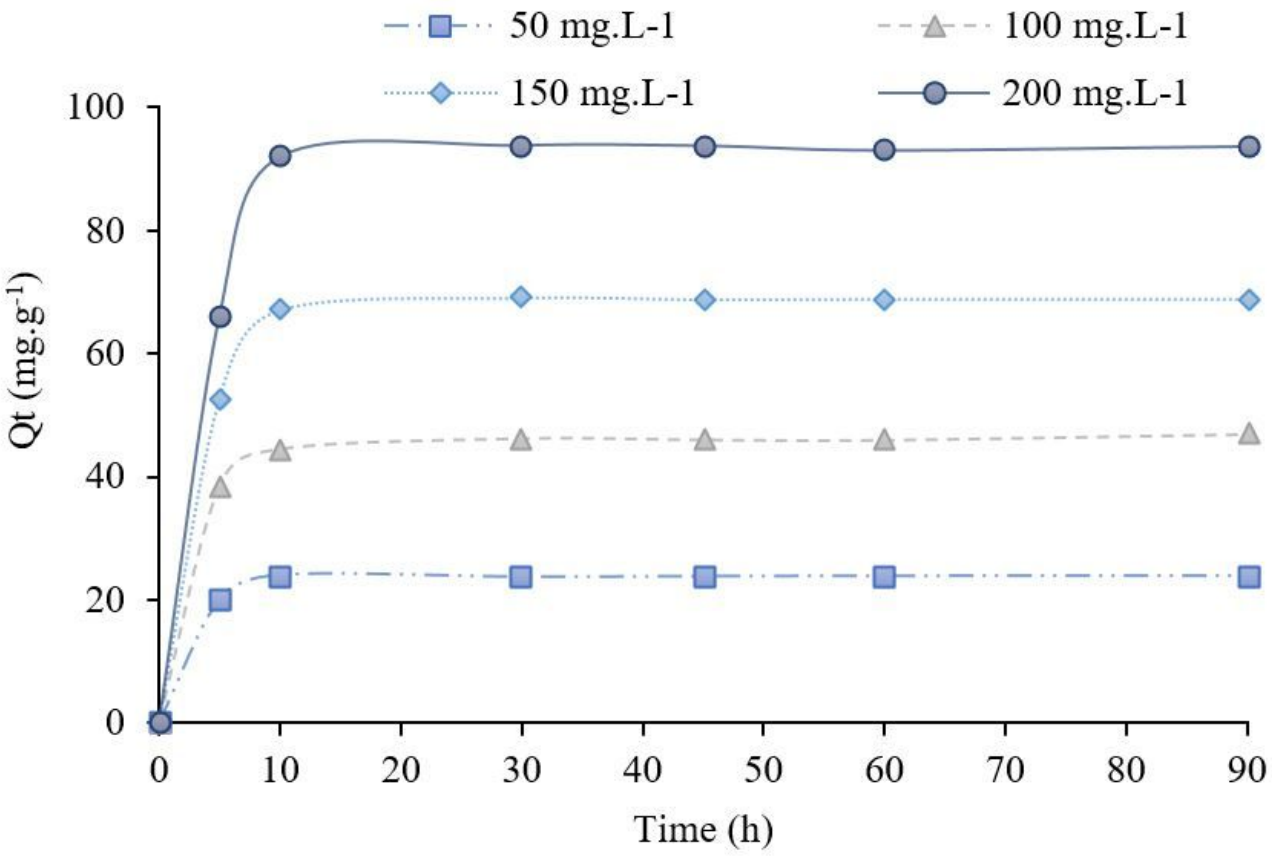

Figure 1

Kinetics of AR14 uptake by W. anomalus biomass at various initial dye concentrations.

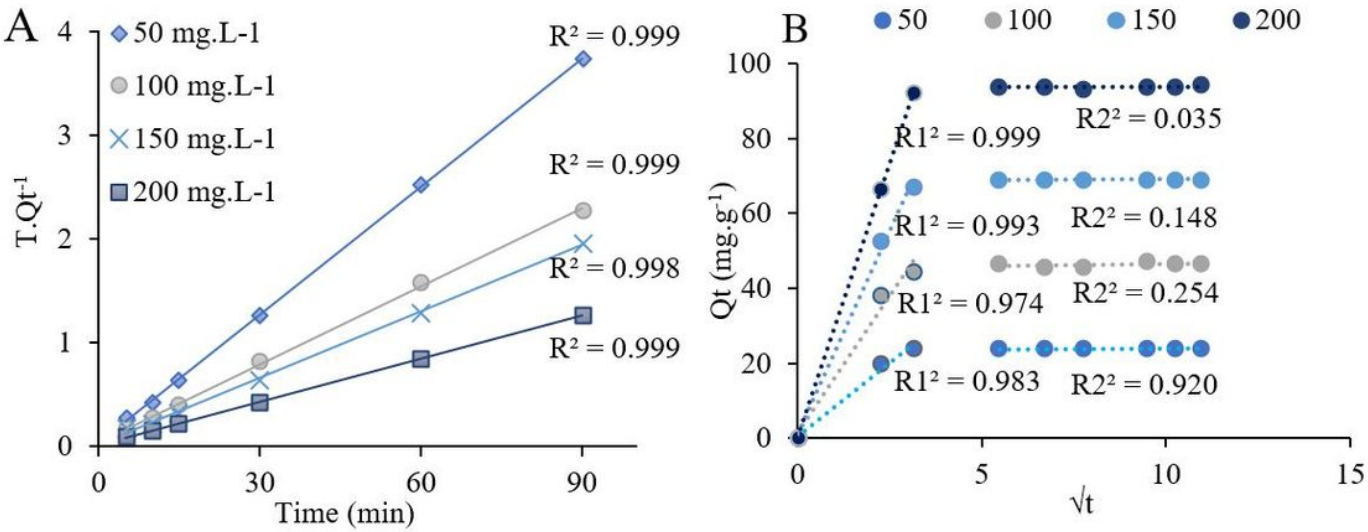

Figure 2

Plot of pseudo-second order model (A), and intra-particle diffusion model (B) of AR14 biosorption onto W. anomalus at various initial concentrations.

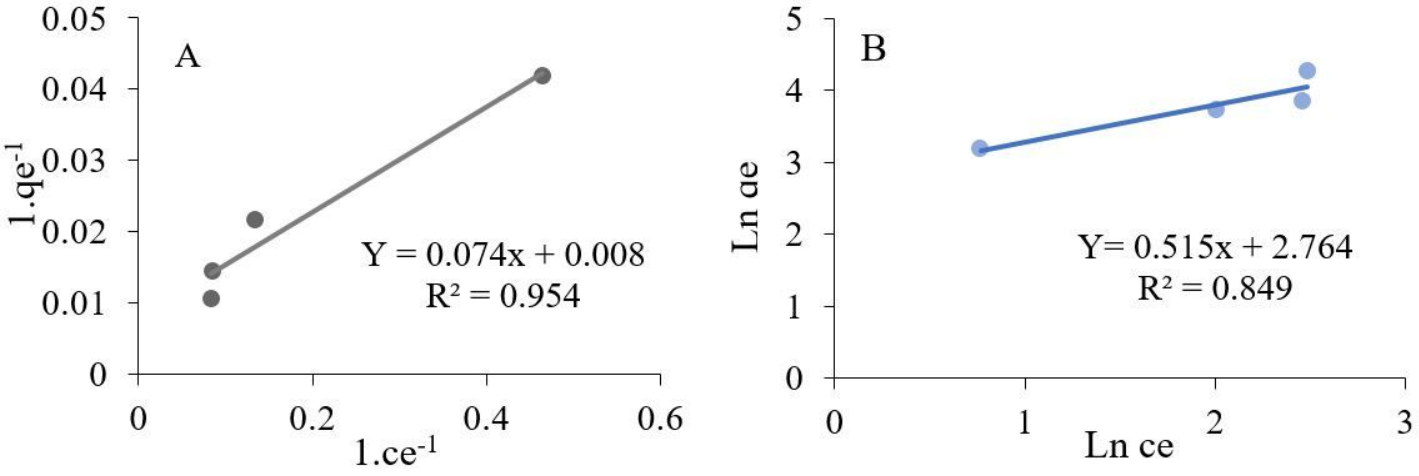

Figure 3

Langmuir (A) and Freundlich (B) isotherm plot and fitted models of AR14 biosorption by W. anomalus biomass.

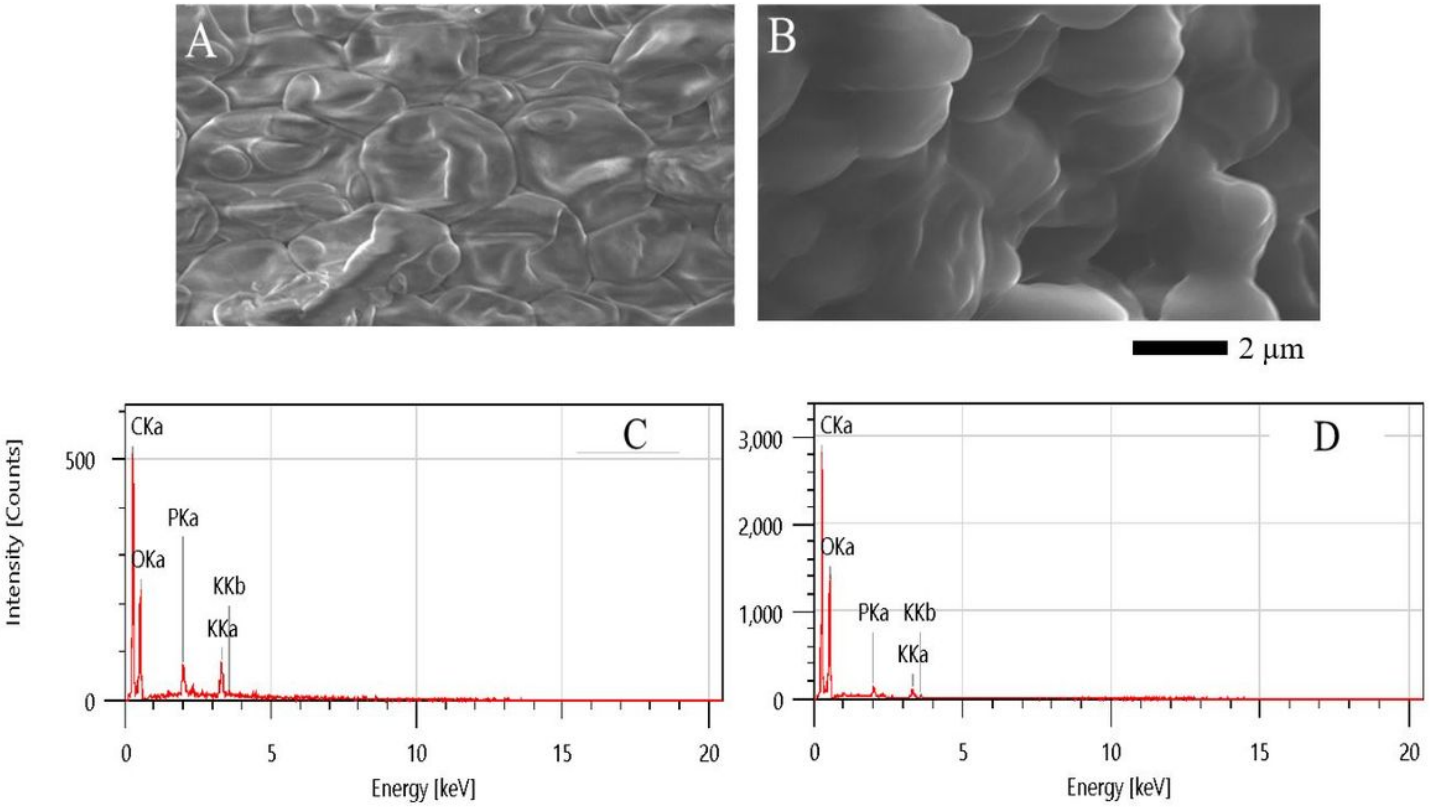

Figure 4

SEM of W. anomalus (x8000): (A) control yeast cells; (B) dye loaded, and the selected X-ray spectra of control (C) and dye loaded cells (D).

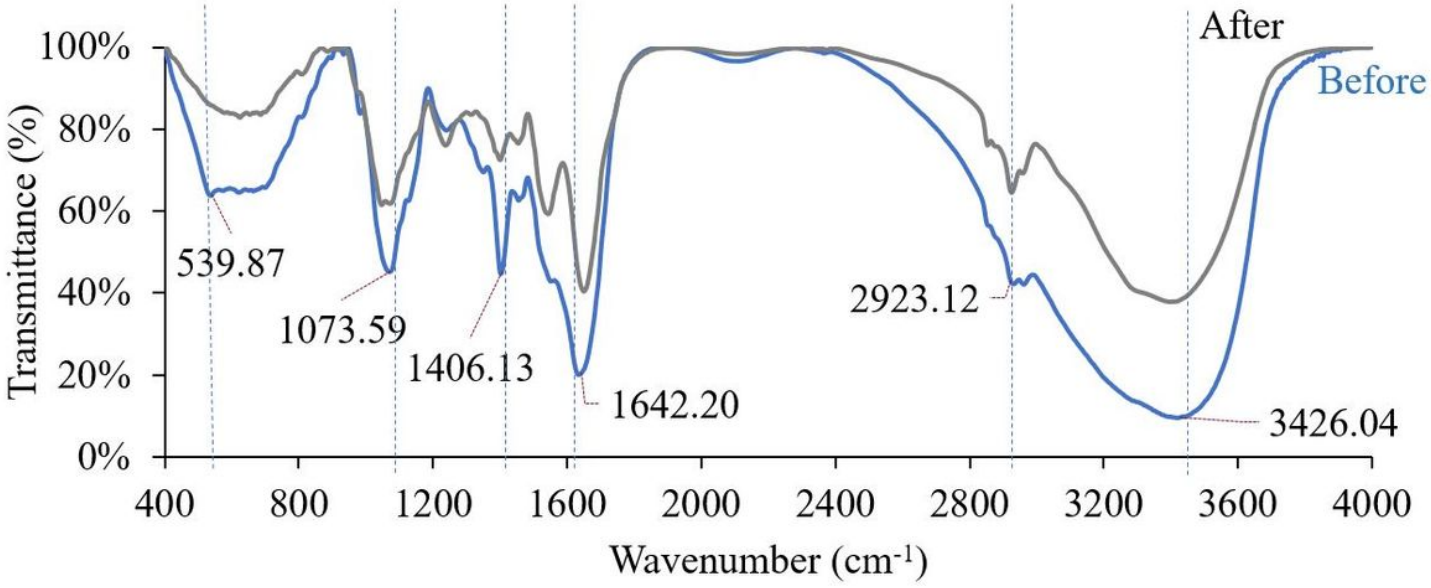

Figure 5

FTIR spectra of W. anomalus cells before and after AR14 biosorption.

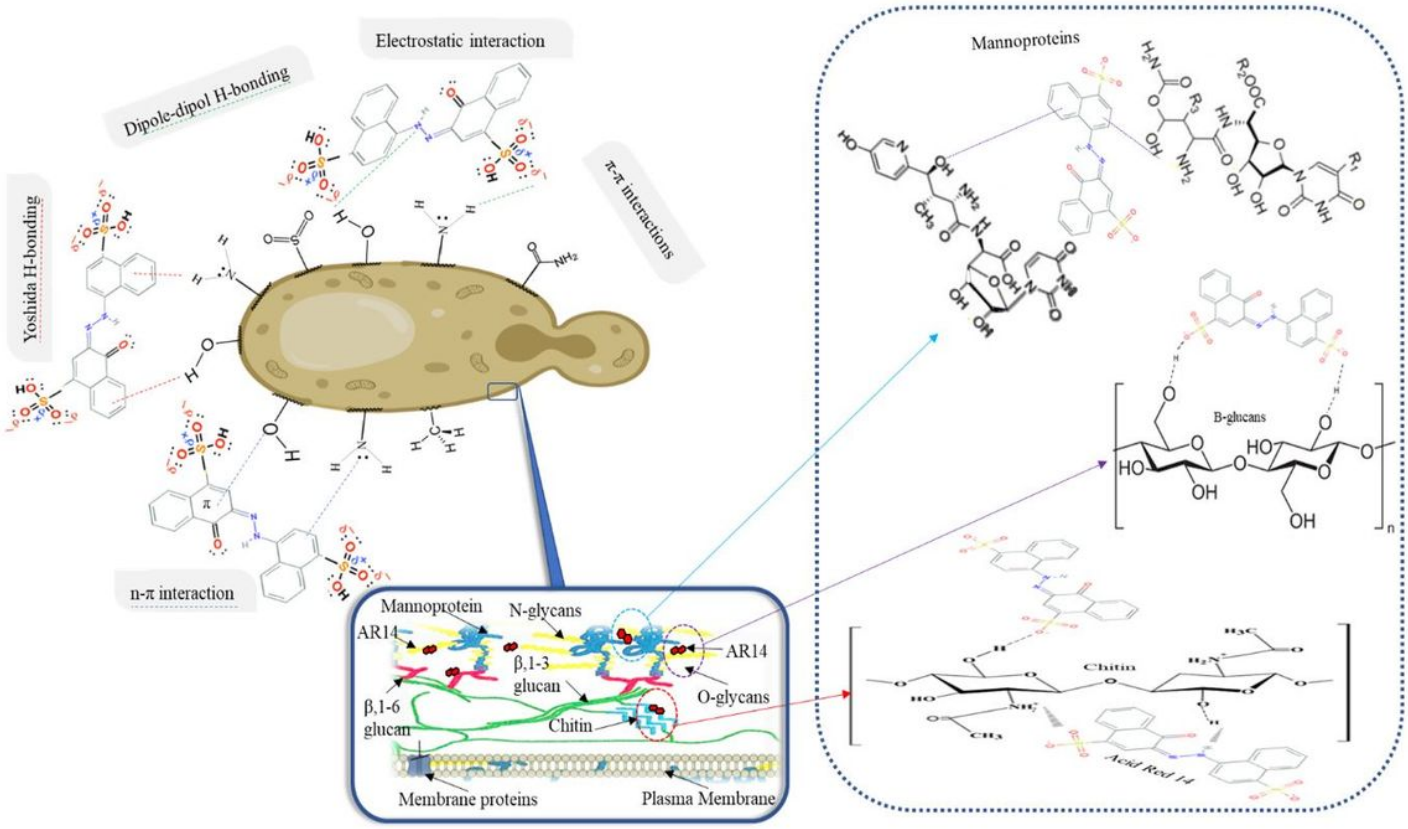

Figure 6

Architecture of yeast cell wall and proposed interaction mechanisms of AR14 biosorption.

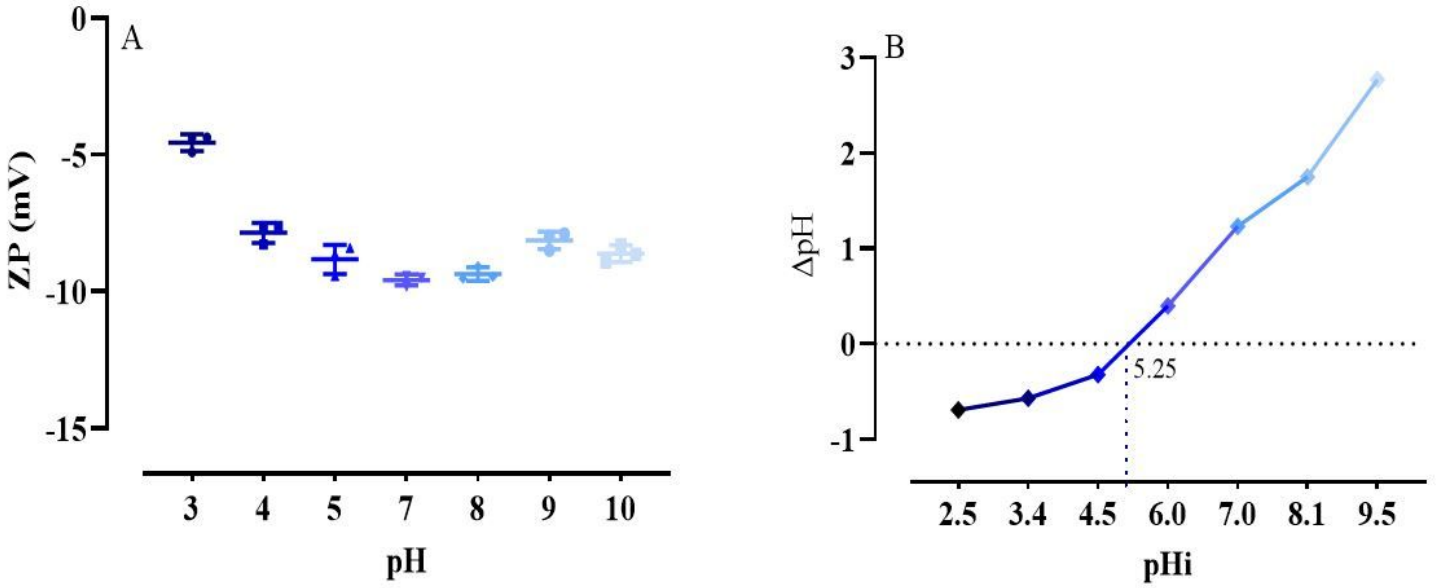

Figure 7

Zeta potential of (A) and pH zero charge (B) of W. anomalus yeast cells

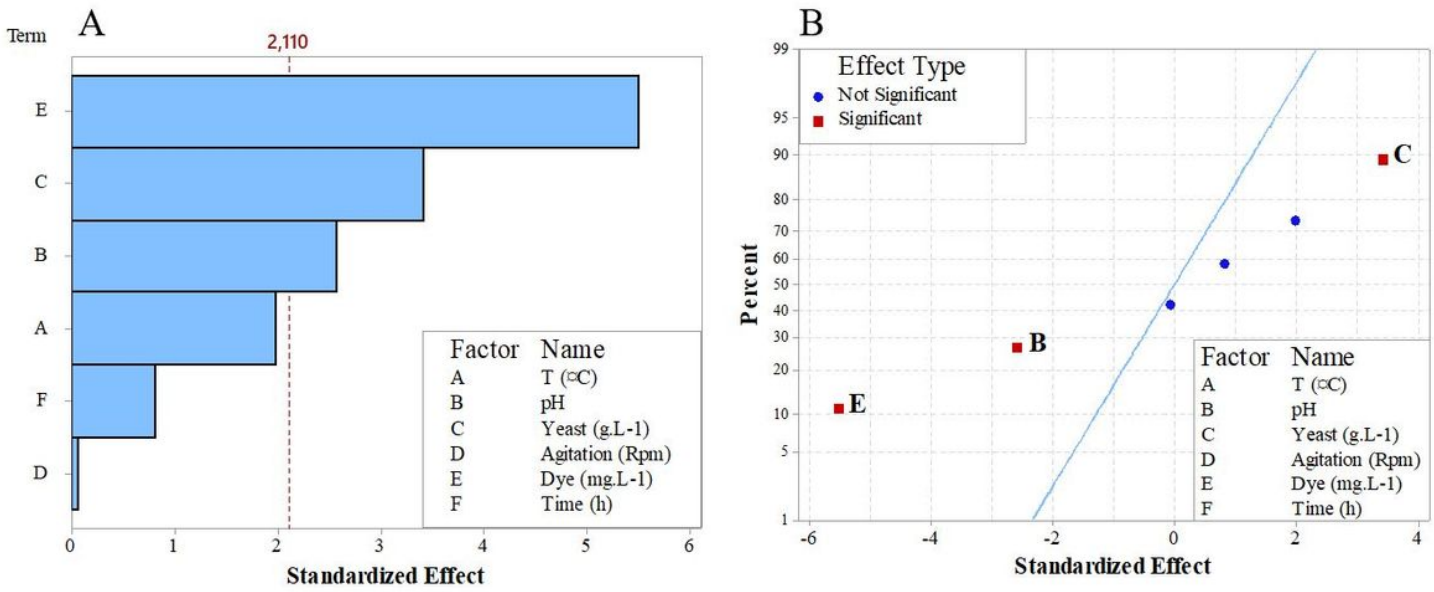

Figure 8

Main effect of variables on the biosorption capacity of AR14 using W. anomalus: Pareto chart of standard effect (A), and normal plot of standardized effects (B).

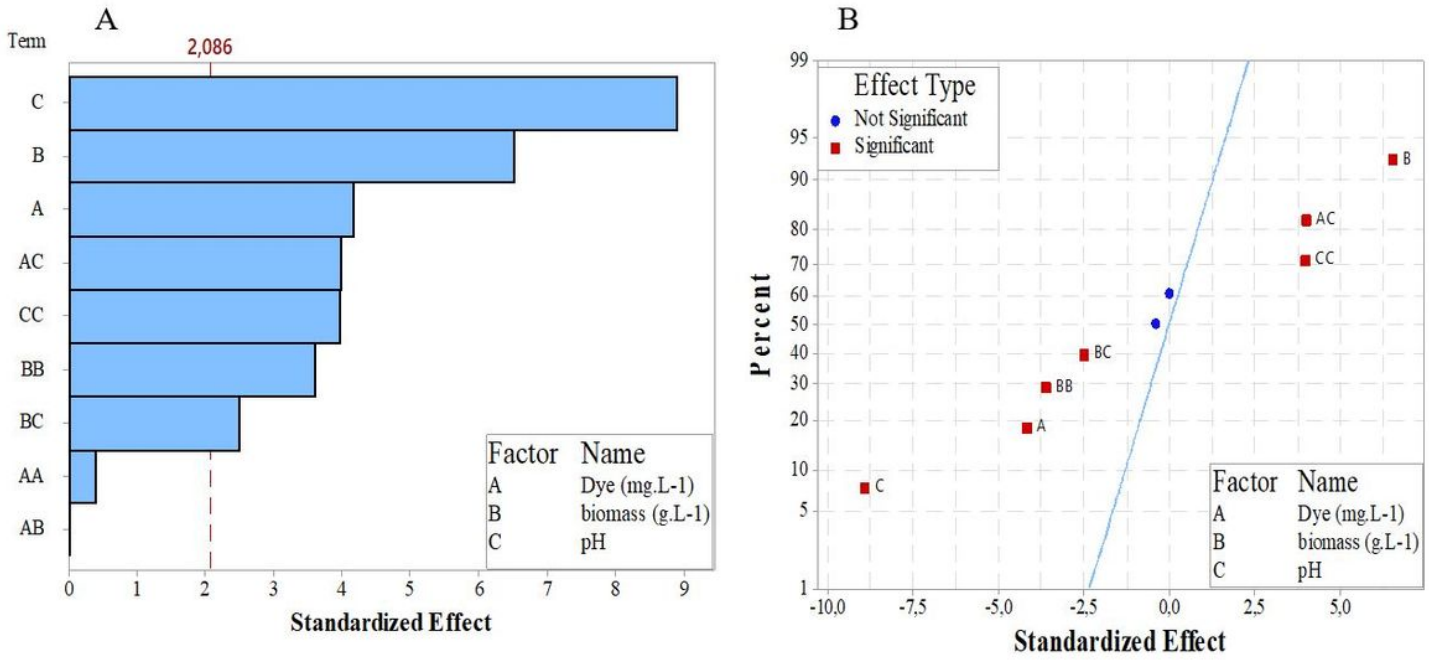

Figure 9

Effect of variables and 2-Way interaction on the biosorption capacity of AR14 using W. anomalus: pareto-chart of standardized effects (A), and normal plot of standardized effects (B).

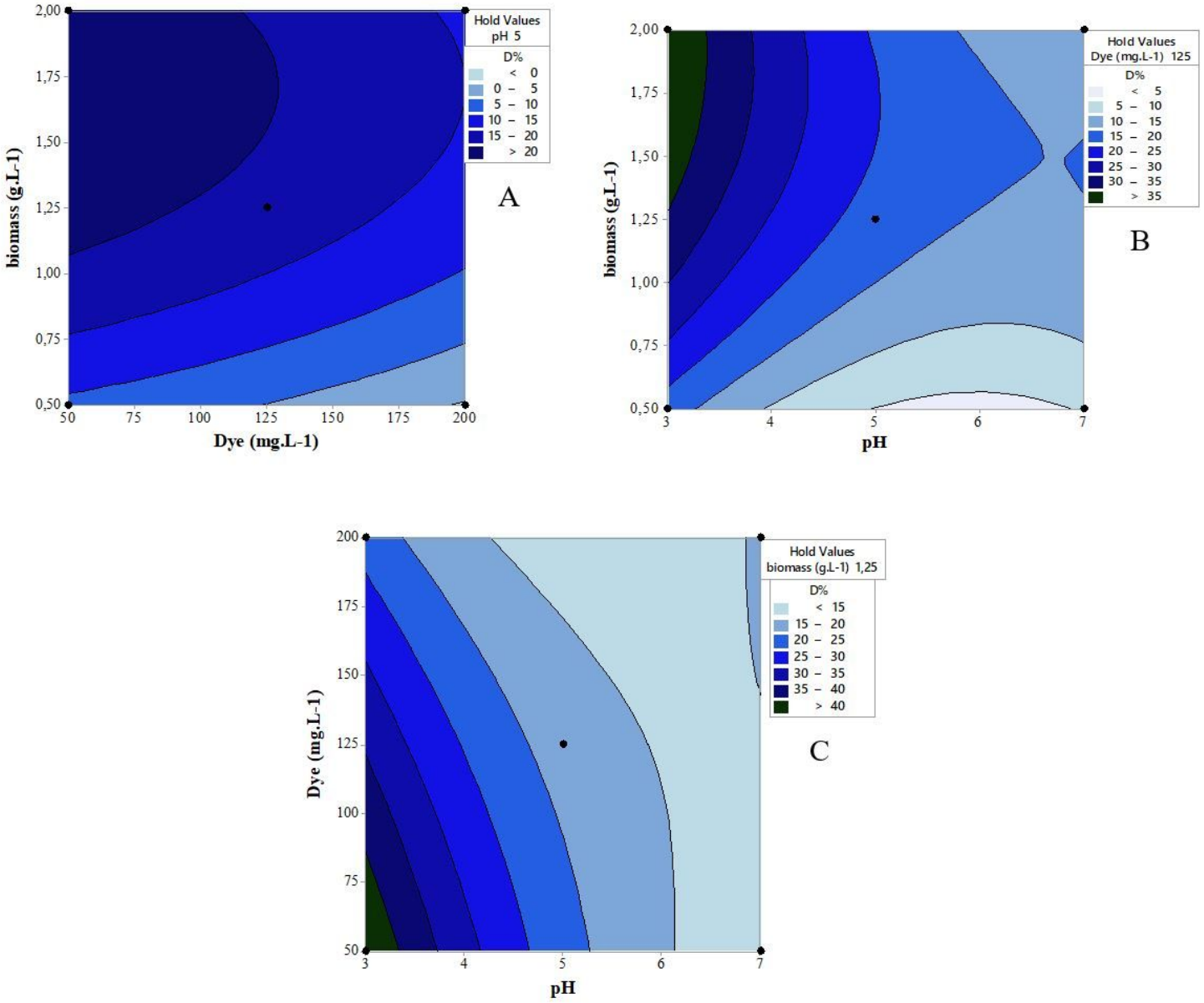

Figure 10

Effect of selected factors (pH, dye concentration and yeast biomass) on the biosorption capacity of AR14 onto W. anomalus.

Supplementary Files

This is a list of supplementary files associated with this preprint. Click to download.

- SupplementaryMaterial.docx